



Higher tree diversity reduces critical slowing down in the Amazon forest

Johanna Van Passel^{1,2}, Koenraad Van Meerbeek^{1,3}, Paulo N. Bernardino^{1,4}, Wanda De Keersmaecker⁵, Stef Lhermitte^{1,6}, Bianca F. Rius^{7,8}, Ben Somers^{1,3}

5 ¹Division Forest, Nature and Landscape, KU Leuven, Leuven, 3001, Belgium.

²Q-ForestLab, Department of Environment, Ghent University, Ghent, 9000, Belgium

³KU Leuven Plant Institute, KU Leuven, Leuven, 3001, Belgium

⁴Department of Plant Biology, University of Campinas, Campinas-SP, 13083-970, Brazil

⁵Flemish Institute for Technological Research (VITO), Mol, 2400, Belgium

10 ⁶Department Geoscience & Remote Sensing, Delft University of Technology, Delft, 2600, Netherlands

⁷Earth System Science Laboratory, Center for Meteorological and Climatic Research Applied to Agriculture, University of Campinas, Campinas-SP, 13083-970, Brazil

⁸Interdisciplinary Environmental Studies Laboratory, Department of Physics, Federal University of Santa Catarina, Florianópolis, SC, 88040-900, Brazil

15 *Correspondence to:* Johanna Van Passel (johanna.vanpassel@ugent.be)

Abstract. The Amazon forest is influenced by strong feedback loops between its biotic and abiotic components. Local forest loss increases CO₂ emissions, which, in turn, drives climate change, raising temperatures and reducing rainfall, causing further forest loss. Additionally, forest loss disrupts important forest-rainfall cycles, threatening the overall forest stability. These feedbacks make the system vulnerable to tipping points, where parts of the forest could transition to a degraded state.

20 Critical slowing down is an early warning indicator for approaching tipping points, as it indicates slower recovery to short-term disturbances. However, the role of tree species diversity in this process is yet to be clarified. Furthermore, it is highly uncertain how the relation between tree species diversity and critical slowing down varies with spatial scales. To examine how tree species diversity impacts critical slowing down across multiple spatial scales, we used modelled tree species diversity data at the alpha (local), beta (asynchrony across local communities), and gamma (regional) scales. We quantified

25 critical slowing down on the same scales using temporal autocorrelation trends in monthly satellite-derived vegetation productivity time series over 2001-2019. Our findings reveal more pronounced slowing down at the alpha level (25 km²) compared to the gamma level (209,903 km²), indicating that Amazonian tipping points are more likely to occur locally than regionally or basin-wide. We also observe significant but weak positive linear relationships between tree species diversity and stability at both alpha and beta scales. This emphasizes both the importance of biodiversity conservation at multiple

30 spatial scales and the complexity of understanding the stability of the Amazon forest.



1 Introduction

Tropical forests play a crucial role in the global carbon cycle. While historically serving as substantial carbon sinks, there is growing evidence that certain tropical forests, including the Amazon, are transitioning to carbon sources (Bennett et al., 2023). This shift is likely attributable to a combination of local and regional disturbances, such as extreme drought events and deforestation (Brienen et al., 2015). Given that forest loss in the Amazon can affect the forest's internal water cycle, leading to further forest loss (Zemp et al., 2017) and global climate change (Artaxo, 2023), these recurrent disturbances could push the Amazon to a tipping point, leading to a change in its functional state (Flores et al., 2024). The stability of the Amazon forest to such disturbances can be quantified using changes in temporal autocorrelation at lag-1 (TAC) of a variable representing an ecosystem state (Boulton et al., 2022). TAC measures the correlation between successive time points in the time series, with an increase indicating a greater similarity between the current and previous ecosystem states over time (Dakos et al., 2012). According to mathematical theory, when dynamical systems such as the Amazon lose stability and approach a tipping point, they are expected to show a slowing recovery to short-term disturbances (translated as an increase in TAC) – a phenomenon known as critical slowing down (Boulton et al., 2022; Scheffer et al., 2009).

The Amazon forest is one of the most biodiverse regions on the planet, with an estimated 16,000 tree species (ter Steege et al., 2020). These species are not equally distributed along the basin due to the observed gradients of environmental conditions including precipitation, seasonality, soil type and fertility, and exposure to disturbance (Luize et al., 2024; ter Steege et al., 2023). The predicted increase in climate change impacts and deforestation across the Amazon could reduce its tree species richness by fifty percent by 2050 (Gomes et al., 2019), but little is known about how these diversity gradients impact critical slowing down in the Amazon forest (Flores et al., 2024; Hutchison et al., 2018). This can be partly attributed to the scarcity of field data on multi-scale tropical tree diversity. However, the emergence of modelled global tree species diversity datasets that cover multiple spatial scales can help to address this (Keil & Chase, 2019; J. Liang et al., 2022). Furthermore, similar to biodiversity patterns, critical slowing down in the Amazon forest might vary significantly from local to regional scales (Keil & Chase, 2019), but this spatial dependency has not yet been quantified (Lenton et al., 2022).

The insurance hypothesis suggests that more diverse ecosystems have a larger buffer against disturbances, owing to the varied species responses to environmental fluctuations (Yachi & Loreau, 1999). Consequently, diversity may increase stability by reducing critical slowing down or the likelihood of tipping points. Empirical support for the diversity-stability hypothesis has been observed in both grassland and forest ecosystems (Isbell et al., 2015; Liu et al., 2022), although contrasting results have been found as well (Grossiord et al., 2014). The relationship between diversity and ecosystem stability has primarily been investigated at local scales (Gonzalez et al., 2020), but diversity can be defined on multiple scales. Alpha and gamma diversity refer to diversity at local and regional scales, respectively, while beta diversity represents differences in diversity across local communities (Buckley & Jetz, 2008; Keil & Chase, 2019). In the Amazon, beta diversity is shaped by biogeographic gradients, such as variations in soil fertility (ter Steege et al., 2006), as well as historical factors, including the long history of plant domestication by pre-Columbian peoples (Levis et al., 2017).



Using a similar rationale, ecosystem stability can be expanded from local (alpha stability) to regional metacommunities (gamma stability) (Wang & Loreau, 2016). In this context, beta stability is defined as the spatial variation in stability responses across local communities, hereafter referred to as spatial asynchrony. Multiple stability frameworks exist, and we adopt the one by Van Meerbeek et al. (2021). Here, stability encompasses all system properties determining the size, length, and irreversibility of changes following a disturbance, including critical slowing down. In other frameworks, this is also referred to as non-local stability or resilience (Dakos & Kéfi, 2022). Combining both frameworks, we anticipate that tree diversity and critical slowing down in the Amazon will relate across multiple scales (Gonzalez et al., 2020; Wang & Loreau, 2016). Based on the insurance hypothesis, we expect a positive correlation between diversity and stability, or a negative correlation between diversity and critical slowing down, at the alpha scale (Liu et al., 2022). On the other hand, there is no defined universal relationship between beta diversity and ecosystem stability. This relationship rather depends on the existing gradients in abiotic heterogeneity, habitat isolation, and species pool richness (Van Der Plas et al., 2023).

In this research, we use changes in TAC of a satellite-derived proxy of canopy productivity as an indicator of critical slowing down, which we combine with modelled tree species richness across multiple spatial scales for the Amazon forest. Our objective is to understand the impact of tree species diversity on critical slowing down of the Amazon, and quantify how this relationship changes across scales. By examining the interplay between diversity and critical slowing down across varying scales, our research aims to advance our understanding of the stability of the Amazon rainforest and shed light on the importance of biodiversity conservation in maintaining ecosystem stability in this critical region.

2 Materials and Methods

2.1 Biodiversity across spatial scales

We used published global maps of modelled tree species diversity at both local and regional scales to investigate their impact on critical slowing down within the Amazon (Keil & Chase, 2019). They integrated data on tree species richness from 1,336 forest plots and 282 countries and other administrative units. Additionally, they included 11 predictors: area, latitude and longitude, biogeographical realm, location on mainland or island, elevation, mean gross primary productivity, mean annual temperature, mean isothermality, seasonality, and precipitation in the driest quarter. All climatic input variables had a spatial resolution of approximately 1 km². Using generalized additive models, they predicted species richness in artificially generated 1-ha plots (alpha diversity plots) and in hexagons spanning 209,903 km² (gamma diversity hexagons) distributed uniformly across the global mainland. Subsequently, 1-ha plots lacking at least one environmental variable and hexagons with less than 50% of mainland area were excluded, resulting in 9,761 alpha diversity plots and 620 gamma diversity hexagons globally. Their model explained more than 90% of the deviance of the data and showed high predictive power when validated with external data. Additionally, they mapped the ratio of gamma and alpha diversity, denoted as beta diversity, at the 1-ha plot scale. Alpha and gamma diversity represent the predicted overall local and regional tree species



95 richness, respectively. Beta diversity indicates the difference in the diversity patterns between both scales, with higher values indicating that a community is relatively less diverse than its surrounding region.

2.2 Stability across spatial scales

In this study, we estimated stability as the absence of critical slowing down, using time series of satellite data across the Amazon (as explained below). The delineation of the Amazon rainforest was adopted from Olson et al. (2001). As a proxy
 100 for the canopy vegetation productivity of tropical forests, we used the enhanced vegetation index (EVI) (Van Passel et al., 2022). EVI measures the canopy greenness, rather than the woody growth response. Therefore, using EVI as a proxy for ecosystem stability assumes that reductions in stem growth coincide with canopy browning (Janssen et al., 2021). We extracted monthly EVI images from 2001 to 2019 from the daily Moderate Resolution Imaging Spectrometer (MODIS) MCD43C4 product with a spatial resolution of 0.05° (Schaaf & Wang, 2015). EVI is calculated using Eq. (1):

$$105 \quad EVI = 2.5 * \frac{(NIR-RED)}{(NIR+6*RED-7.5*BLUE+1)}, \quad (1)$$

where NIR, RED and BLUE are the surface reflectance values of the near-infrared, red and blue MODIS bands, respectively. Pixels with a low Bidirectional Reflectance Distribution Function (BRDF) inversion quality (50% or more fill values) or classified as outliers were excluded from the time series. Additionally, pixels with over 10% missing values in their time series were masked. We minimized the potential impact of anthropogenic factors on the stability of the Amazon rainforest by
 110 excluding areas that were categorized as non-native forest landscapes (Potapov et al., 2008), with a tree cover below 60% (DiMiceli et al., 2015), and those subjected to burning from 2001 to 2019 (Giglio et al., 2015).

To assess the regional (gamma) stability response, we first calculated the mean EVI time series for all non-masked 0.05° pixels within the gamma diversity hexagons outlined by Keil and Chase (2019). Subsequently, for each hexagon, the mean EVI time series were detrended and deseasonalized using STL decomposition (seasonal and trend decomposition using
 115 Loess; Cleveland et al. (1990)), resulting in EVI remainder time series. The calculations for the long-term trend and the seasonality used time windows of 19 and 13 months, respectively (Van Passel et al., 2024a). The decomposed EVI remainder was then used to calculate the lag-1 autocorrelation with a moving window length of five years. The trend in TAC was determined as the slope of the linear regression of the TAC time series from 2001 to 2019, and was used to quantify regional critical slowing down. For ease of interpretation (i.e., higher values denote higher stability), we used the negative
 120 value of the slope in TAC as the gamma stability value. Negative gamma stability values thus indicate an increase in TAC over the 20-year period, indicating decreased stability, and vice versa.

The modelled alpha and beta diversity plots from Keil and Chase (2019) are spatially distributed point values at regular intervals of approximately 82 km. To integrate this data with the pixel-based 0.05° satellite time series, we established a buffer zone surrounding the diversity plots to determine which satellite pixels corresponded to specific diversity values. To
 125 assess their robustness, multiple buffer zones of varying sizes were employed. Specifically, buffer zones with radii of 8.5 km (size of 225 km²), 14.1 km (625 km²), and 19.7 km (1,225 km²) were utilized to match the area of three by three, five by five,



and seven by seven MODIS 0.05° EVI pixels, respectively. Within each buffer zone, all pixels were assigned the same alpha and beta diversity values. In the analysis using the smallest buffer size of 225 km², a total of 1,866 EVI pixels within 497 buffer zones were considered. These numbers expanded to 5,130 and 9,904 EVI pixels in 551 and 591 buffer zones when using the larger buffer sizes of 625 and 1,125 km², respectively (Table A1).

Using the same methodology as for the gamma scale, alpha stability was derived as the negative value of the TAC trend in the EVI time series of the pixels included in a buffer zone. Spatial asynchrony (or beta stability) indicates the spatial variability in stability responses within a region. To estimate it, we followed the definition of beta diversity by Keil and Chase (2019), and calculated it on the local scale for all pixels within a buffer zone using Eq. (2):

$$135 \quad \text{Spatial asynchrony} = \frac{\text{Gamma stability} + 0.1}{\text{Alpha stability} + 0.1}, \quad (2)$$

Given that both gamma and alpha stability values varied between approximately -0.01 and 0.01, we added 0.1 to both stability metrics to ensure that both the numerator and denominator are always positive. A spatial asynchrony value above one indicates lower local stability compared to the stability of the surrounding region, while a value below one indicates a relatively higher local stability compared to the regional stability. This transformation of adding a constant to both numerator and denominator is necessary to avoid having a positive gamma and negative alpha stability value or a negative gamma and positive alpha stability resulting in the same spatial asynchrony value. However, to quantify whether this transformation shifts the ratio away from representing the true proportional relationship between regional and local stability, we also split our dataset into those with strictly positive or negative alpha stability values. For each category, we also calculated spatial asynchrony as the ratio of gamma and alpha stability without adding a constant, and these results are presented in Appendix A.

Apart from increasing TAC, another potential indicator of critical slowing down is an increase in the variance of the system's state variable (Ditlevsen & Johnsen, 2010; Scheffer et al., 2009). To quantify the trend in variance, we calculated the standard deviation (SD) of the remainder of the decomposed EVI time series with a moving window of five years. We calculated alpha and gamma stability using only the 0.05° pixels that showed a consistent positive or negative trend for both TAC and SD, following the theory that an increase in TAC cannot serve as evidence of slowing down if there is no corresponding increase in variance (Ditlevsen & Johnsen, 2010). We repeated all analyses below using only the subset of pixels with consistent trends to provide a more nuanced understanding of the stability dynamics of the Amazon forest (see Appendix A).

2.3 Environmental heterogeneity

To account for the diverse conditions within the Amazon forest, we incorporated different environmental variables known to impact how tropical forests respond to perturbations. As topography modulates the embolism resistance of tropical tree species (Mattos et al., 2023), we included elevation (from NASA JPL (2013)). Additionally, information on the soil sand and clay content from Poggio et al. (2021) was integrated, as soil texture influences the water infiltration speed and water



retention capacity of the soil (Van Passel et al., 2022). Lastly, we included seasonality to describe the precipitation variability in the Amazon forest, derived from the monthly TerraClimate dataset from 1980 to 2019 (Abatzoglou et al., 2018), calculated using the Seasonality Index (Walsh & Lawler, 1981). We took the mean value of each environmental variable per 0.05° pixel and 209,903 km² hexagon to include in the following analyses.

2.4 Extreme drought occurrences

Extreme drought occurrences are prevalent perturbations in tropical forests (IPCC, 2021). Therefore, we also included variables characterizing the drought history of each pixel. Extreme drought occurrences were identified spatially and temporally using cumulative water deficit (CWD) anomalies (Van Passel et al., 2022). CWD was calculated for all pixels within the Amazon using TerraClimate precipitation (P) time series from 1980 to 2019 (Abatzoglou et al., 2018), and assuming a fixed evapotranspiration (E) of 100 mm per month, using the following rule (Aragão et al., 2007):

If $CWD_{n-1} - E + P_n < 0$;

Then $CWD_n = CWD_{n-1} - E + P_n$;

Else $CWD_n = 0$

Where n represents each month in the time series. CWD represents periods when monthly precipitation is insufficient to offset both the evaporation occurring that month and any precipitation shortfall carried over from the previous month. The CWD dataset was then used to calculate the mean and standard deviation of CWD per month. Standardized anomalies were determined per 0.05° pixel by subtracting the monthly mean from the pixel value and dividing the result by the monthly standard deviation. Pixels with CWD anomalies below -1.96 were significantly drier than average (with $p < 0.05$). Extreme drought periods were defined as starting with at least two months of significantly dry CWD anomalies and ending when the anomaly became positive. Since a fixed evapotranspiration value was used, the CWD anomalies in this study represent meteorological droughts rather than hydrological droughts. For each drought event, the intensity was calculated as the absolute value of the minimal CWD anomaly value during the drought period, while the duration was defined as the number of months that the drought lasted. The drought history of each pixel was then characterized using drought frequency (i.e., the number of separate drought events between 2001 and 2019), along with the average drought intensity and duration of all occurred droughts.

2.5 Diversity-stability relationship across spatial scales

All analyses were performed using the R statistical environment (R version 4.2.3; R Core Team, 2021). Using the R package piecewiseSEM (Lefcheck, 2016), piecewise structural equation modelling was used to explore the relationships between environmental factors, drought-related variables, diversity, and stability across various spatial scales, considering each buffer size. We first constructed a conceptual model, where we hypothesized a negative relationship of local diversity with critical slowing down, or a positive relationship with stability, because of the expected buffering effect of higher diversity against disturbances (Fig. 1) (Liu et al., 2022; Wang & Loreau, 2016). Furthermore, we anticipated that the spatial variability in



stability responses between local communities (i.e., spatial asynchrony) would be driven by the spatial variability in diversity between them (i.e., beta diversity). Lastly, we expected spatial asynchrony to exert a more pronounced positive impact on gamma stability than local stability. This expectation stems from the high spatial heterogeneity and species turnover characterizing the Amazon forest (Keil & Chase, 2019; Qiao et al., 2022).

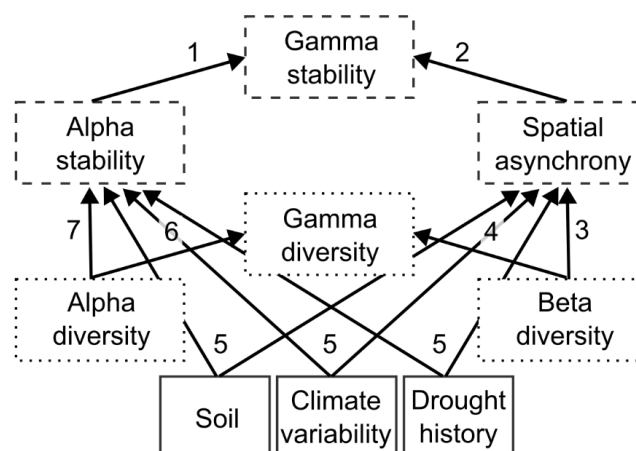


Figure 1: Conceptual model with hypotheses for all causal relationships in the structural equation model. The dashed boxes represent stability across spatial scales, while the dotted boxes represent the diversity components. The different hypotheses are: (1) A region will be more stable if it contains more stable communities; (2) A region will be more stable due to higher spatial variability in stability responses between communities; (3) Spatial variability in stability responses will be driven by the spatial variability in diversity; (4) A region will be more diverse due to higher spatial variability in diversity between pixels; (5) Soil, climate variability, and drought-related variables will impact local stability and spatial asynchrony; (6) A region will be more diverse if it contains more diverse communities; and (7) A community will be more stable if it is more diverse due to the insurance hypothesis.

The structural equation model incorporated three linear mixed-effects models with an exponential spatial autocorrelation structure to model the diversity-stability relationship on the alpha, beta, and gamma scales, using the R package nlme (Pinheiro et al., 2021). The models met all the assumptions of a linear model, that is, linearity of the data, normality of the residuals, homogeneity of residuals variance, and independence of the error terms. Considering that all alpha stability values within a given buffer zone shared the same alpha diversity value, “buffer zone ID” was included as a random effect in the alpha and gamma stability models. Additionally, for the beta-scale model, where beta diversity and spatial asynchrony were computed using a single gamma value per region, both “buffer zone ID” and “region ID” were included as nested random effects. We also included a generalized mixed-effects model for the diversity relationship across scales in the structural equation model, with “region ID” as a random effect and a Poisson distribution for the gamma diversity data, using the R package MASS (Venables & Ripley, 2002). We included multiple climatic and soil variables known to influence the stability of the Amazon to disturbances, along with variables describing the extreme drought history of each pixel (see above), as an example of a recurring disturbance within the Amazon forest. However, seasonality was not included directly in the alpha stability model due to its high variance inflation factor when combined with alpha diversity. Therefore, we included seasonality as a covariate of alpha stability instead. To test the robustness of the modelled diversity data, we also repeated



the alpha-scale diversity-stability analysis using two other publicly available tree species diversity datasets (J. Liang et al., 2022; ter Steege et al., 2023), with the results included in Appendix A.

220 3 Results

When including only the satellite pixels overlapping with the regularly distributed alpha diversity plots, we observed negative stability values, or areas experiencing critical slowing down, for 40% of the included EVI pixels at the alpha scale and for 20% of the regions at the gamma scale (Fig. 2 and Fig. 3). Additionally, more than 70% of the EVI pixels exhibited a spatial asynchrony value above one, indicating a relatively stronger critical slowing down tendency in the local forest communities than in the larger region where they are situated.

Consistent with our hypotheses, we found significant but weak positive linear relationships between diversity and stability on both the alpha scale (marginal $R^2 = 0.01$, conditional $R^2 = 0.18$) and the beta scale (marginal $R^2 = 0.02$, conditional $R^2 = 0.41$) (Fig. 3 and Fig. 4, Table A1). However, we did not find a significant relationship on the gamma scale when accounting for spatial autocorrelation (Fig. 3). These significant relationships on the alpha and beta scale persisted when using larger buffer sizes, and when restricting the analysis to only pixels with consistent TAC and SD trends (Table A1 and A2). We also found a significant positive relationship between alpha stability and diversity for the globally modelled tree species diversity dataset from Liang et al. (2022), but no significant relationship with the Amazon-based diversity estimates (Fig. A2).

Moreover, we found significant positive effects of both alpha stability and spatial asynchrony on gamma stability, with spatial asynchrony having a slightly larger effect size (Fig. 4). Notably, local environmental conditions and drought history variables did not exert significant effects on alpha stability. In contrast, precipitation seasonality, elevation, and drought frequency did significantly impact spatial asynchrony. When incorporating larger buffer sizes or when restricting the analysis to the pixels with consistent TAC and SD trends, most of these significant relationships remained robust (Fig. A3 and A4). Furthermore, higher soil sand content was found to significantly increase alpha stability in many of these models. When splitting the dataset into negative and positive alpha stability values to avoid the use of the constant in Eq. (2), the larger effect size of spatial asynchrony on gamma stability compared to that of alpha stability remained robust, as did the impact of precipitation seasonality on spatial asynchrony (Fig. A5). We also found positive impacts of alpha and beta diversity on alpha stability and spatial asynchrony, respectively, when only including the positive alpha stability values, although the impact of beta diversity became insignificant for the negative alpha stability values.

245

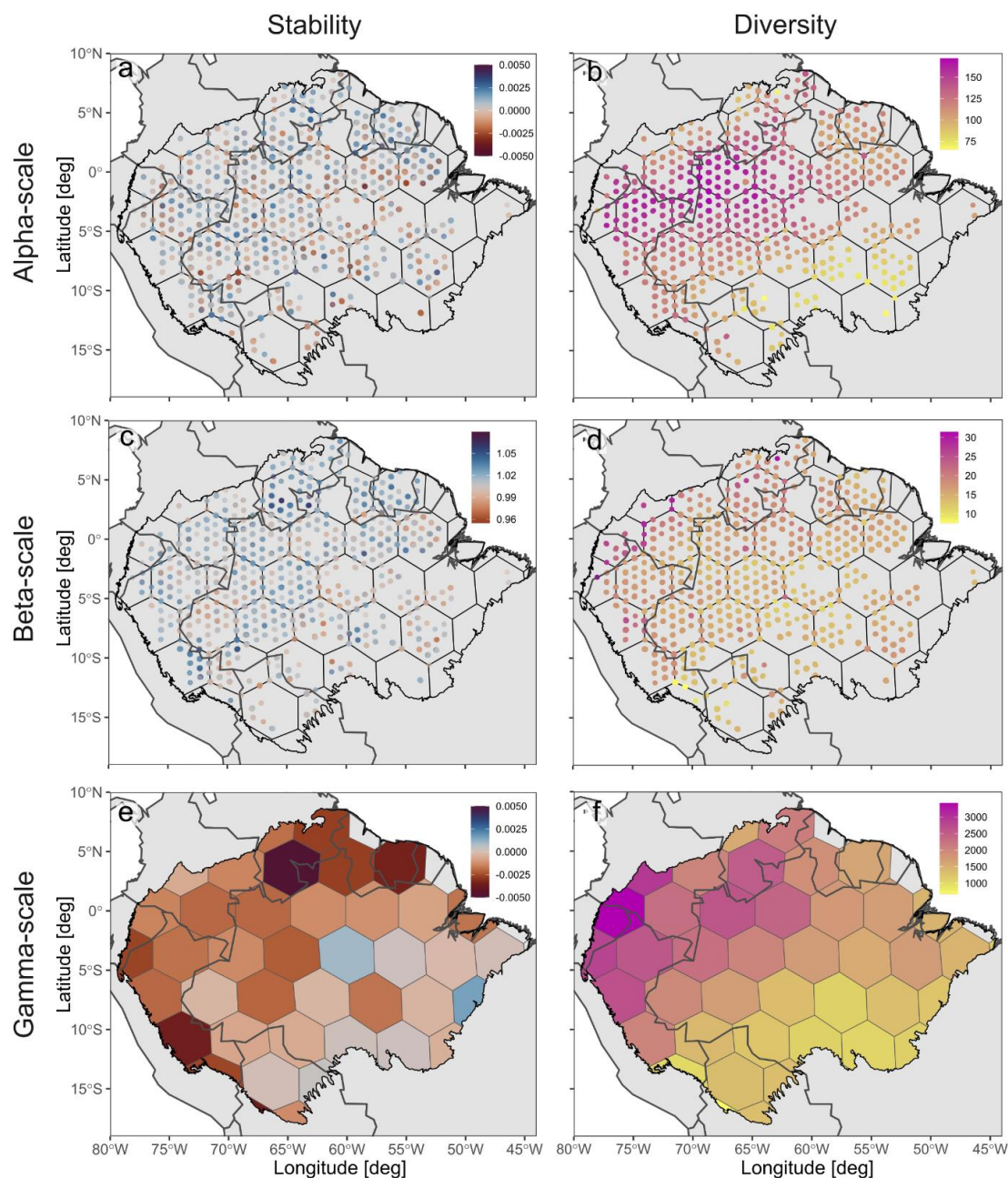


Figure 2: Stability (i.e., the negative TAC trend) and diversity (i.e., modelled tree species richness) for the Amazon region across spatial scales using the smallest buffer size of 225 km². (a and b) Alpha stability and diversity; (c and d) spatial asynchrony and beta diversity; and (e and f) gamma stability and diversity. In (a) and (c), the individual pixels are shown bigger than their real size for increased visibility. The original maps are shown in Fig. A1.

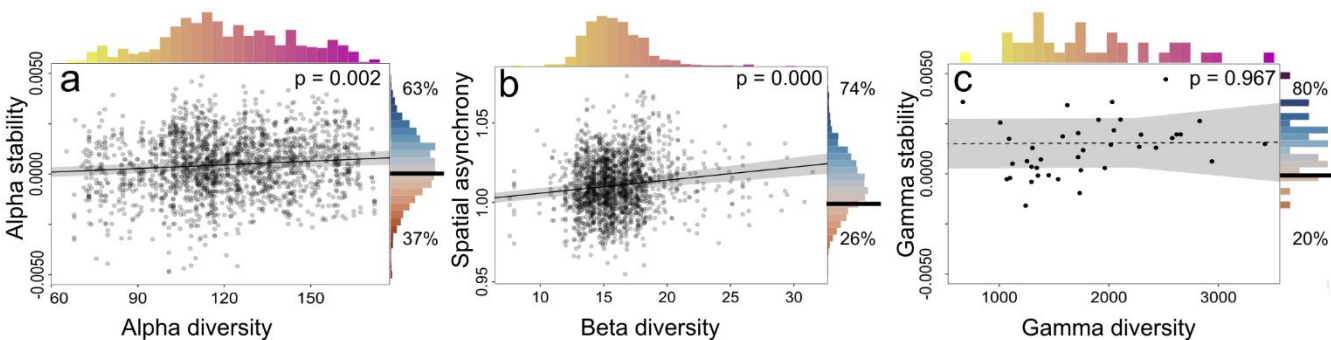


Figure 3: Linear diversity-stability relationships on the (a) alpha, (b) beta, and (c) gamma scale, for the smallest buffer zone of 225 km². The lines in (a) and (b) show significant positive relationships while considering random effects and spatial autocorrelation ($p < 0.05$), while (c) does not have a significant relationship. The histograms on the top and the right side show the distribution of the diversity and stability values, respectively, following the colour scale of Fig. 2. The black lines in the right histograms indicate zero in (a) and (c), and 1 in (b), with the percentage of values above and below.

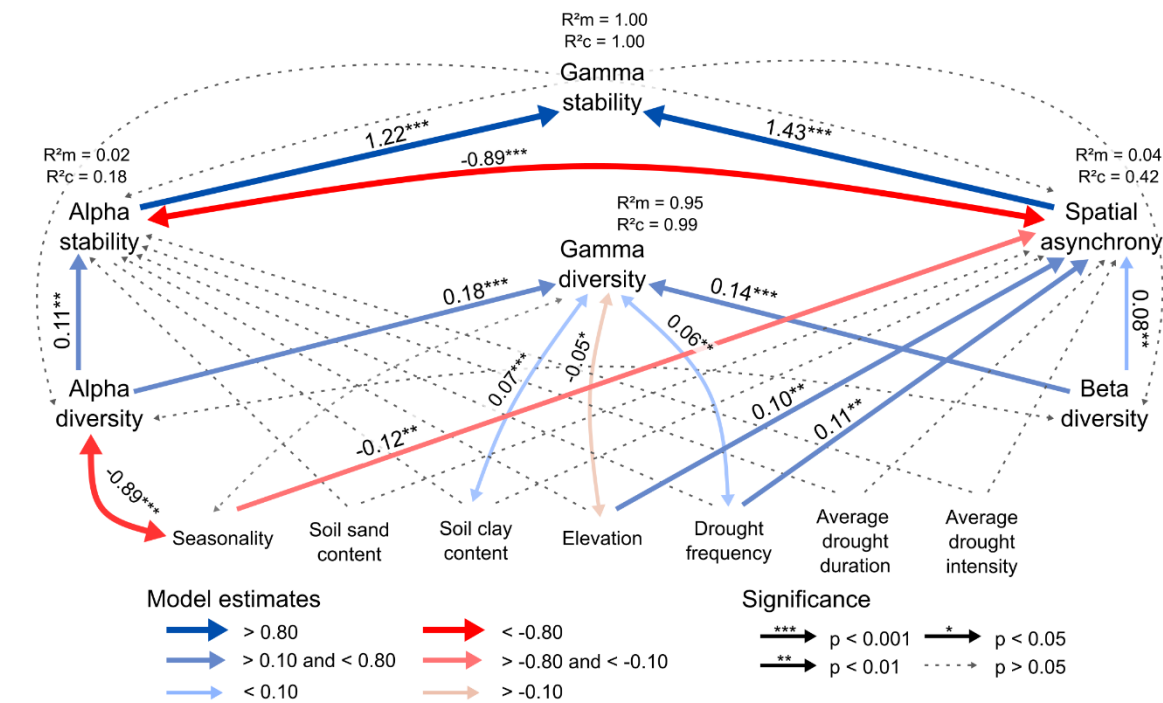


Figure 4: Representation of the structural equation model involving the causal relationships between stability, diversity, environment, and drought history across spatial scales, using the smallest buffer size of 225 km². Model Fisher's $C = 41.4$ ($p = 0.08$). The R^2m and R^2c values next to the response variables represent the marginal and conditional R^2 values, respectively. The single-headed straight arrows represent causal pathways, and the double-headed curved arrows represent the covarying variables. The numbers on the arrows represent the significant effect sizes of the standardized path coefficients.



4 Discussion

265 We integrated changes in satellite-derived TAC of canopy productivity with modelled tree species richness to understand
the impact of tree species diversity on critical slowing down of the Amazon forest. By incorporating stability and diversity
data across multiple spatial scales, we showed that forest areas characterized by higher alpha tree species diversity exhibit
less critical slowing down. More diverse forest communities thus tend to be further away from a potential critical threshold
to a degraded state. Additionally, communities with greater dissimilarity in tree species composition (i.e., higher beta
270 diversity) contribute to increased heterogeneity in stability responses across the region, confirming the positive diversity-
stability relationship in the Amazon at both alpha and beta scales. This highlights the critical role of biodiversity
conservation in upholding ecosystem stability within the Amazon forest. However, the low R^2 values of the positive
relationships also show the complexity of understanding the drivers of ecosystem stability in the Amazon forest.

4.1 Critical slowing down of the Amazon forest vegetation

275 Our analysis reveals that approximately one-third of the analyzed pixels within the Amazon forest exhibited local slowing
down over the 20-year study period, which decreases to one-fifth of the Amazon at the regional scale. This aligns closely
with the findings of Van Passel et al. (2024) for the entire Amazon, indicating that the subset of pixels investigated in this
study can be considered representative of the broader Amazon rainforest. Additionally, more than 70% of the EVI pixels
displayed a spatial asynchrony value above one, indicating a relatively stronger tendency of slowing down locally than
regionally. This disparity can possibly be attributed to significant variations in environmental conditions, including
280 topography, microclimate and soil types, at the local scale (Ismaeel et al., 2024; Mattos et al., 2023; Zuquim et al., 2023).
Such variations likely contribute to greater variability, leading to a higher incidence of local slowing down. In contrast, the
analysis at the regional scale may smooth out these local differences, making broader regional patterns of the region more
apparent and resulting in less pronounced regional slowing down. This observed pattern of increased stability from the local
285 to the regional levels parallels findings in research on drought resistance across spatial scales in the Amazon (Janssen et al.,
2020). It underscores the importance of considering various spatial scales when investigating ecosystem stability.
Furthermore, this pattern also suggests that the Amazon is more likely to experience local transitions to a degraded state than
to reach a regional or system-wide critical threshold.

4.2 Diversity-stability relationship across spatial scales

290 The significant diversity-stability relationships on the alpha and beta scales highlight the role of tree species diversity and its
spatial heterogeneity in protecting the Amazon forest from reaching a tipping point. However, the low explanatory power of
these relationships could potentially be due to the high functional redundancy in Amazonian forests. At small scales,
additional species can still make a difference in terms of niche complementarity, whereas, at larger spatial scales, they may
lead to functional redundancy (Poorter et al., 2015).



295 The observed positive relationship between local diversity and stability is consistent with the insurance hypothesis. Higher species diversity promotes diversity of responses to various local disturbances, mitigating the overall impact on local communities, and thereby, lowering the chances of the forest to transition into a degraded state. This positive relationship is in line with prior research investigating stability of (sub)tropical forests, where stability was quantified as either a lack of slowing down, resistance to drought events, or temporal stability of productivity (Hutchison et al., 2018; Liu et al., 2022; 300 Ouyang et al., 2021).

The significant positive relationship between beta diversity and spatial asynchrony indicates that communities with greater dissimilarity in composition contribute to increased heterogeneity in stability responses across the region, a phenomenon referred to as the spatial insurance effect (Wang & Loreau, 2016). While there has been less research on this relationship compared to the alpha scale, especially in tropical forests, empirical evidence in temperate biomes has also demonstrated the 305 existence of the spatial insurance effect (M. Liang et al., 2022; Qiao et al., 2022). Beta diversity is especially important in driving ecosystem functioning in abiotically heterogeneous landscapes (Van Der Plas et al., 2023). The Amazon forest is a clear example of such a landscape, with its highly diverse soils shaped by a complex geological history (Hoorn et al., 2010; Tuomisto et al., 2019), and further influenced by variations in precipitation seasonality and local topography that strongly influence local hydrological conditions (Costa et al., 2023; Mattos et al., 2023).

310 The absence of a significant causal relationship between diversity and stability on the regional scale aligns with previous findings in temperate ecosystems (Hautier et al., 2020; Qiao et al., 2022), but contradicts other findings (M. Liang et al., 2022). This lack of significance could be due to the small sample size (Figure 3c), which could hide any possible real effect due to low statistical power. At the same time, in a meta-analysis of observed drought responses in the Amazon, regional-scale drought responses of productivity were also reported to be of smaller magnitude and significance compared to those on 315 the local scale (Janssen et al., 2020). At the regional scale, aggregating local dynamics often leads to a smoothing of temporal variability, as asynchronous responses among local communities can offset each other. This attenuation of change magnitudes, combined with high functional redundancy, may buffer regional-scale ecosystem functioning and thus weaken the apparent strength of diversity–stability relationships. As a result, even substantial changes at the local scale may translate into smaller, less detectable effects when averaged over large areas. This, in combination with the relatively low R^2 values 320 observed between diversity and stability on both the alpha and beta scales, emphasizes that positive relationships between species richness and stability tend to be weak in tropical forests and diminish with increasing spatial scales (Ouyang et al., 2021; Qiao et al., 2022).

4.3 Environmental and climatic drivers

Our study also revealed significant effects of various environmental and drought-related variables on stability at both the 325 alpha and beta scales. Specifically, more sandy soils were associated with less local slowing down, following earlier findings demonstrating higher drought resistance on more sandy soils in the Amazon forest (Van Passel et al., 2022). While this result may seem surprising, given that higher sand content typically correlates with lower nutrient availability and higher



aluminium saturation (Laurance et al., 1999), it might be attributed to the higher hydraulic margin of tree species in low-resource environments (Oliveira et al., 2021).

330 Similarly, spatial asynchrony was significantly influenced by multiple variables. Firstly, it was lower in more seasonal forests within the Amazon, indicating that more seasonal forest communities exhibit relatively less slowing down compared to the larger region where they are located. Conversely, forest communities located at higher elevations or experiencing more drought events in the 20-year period showed higher spatial asynchrony. Existing literature suggests negative impacts of all three variables – seasonality, elevation, and drought frequency – on local tropical forest stability (Liu et al., 2022; Mattos
 335 et al., 2023; Ouyang et al., 2021; Van Passel et al., 2022). However, our data reveals interesting nuances in how these impacts on critical slowing down of the Amazon forest change when increasing the spatial scale (Fig. A6). Notably, the impact of higher seasonality becomes more negative (although non-significant) when increasing the spatial scale, which could be attributed to the gradual changes in seasonality over large spatial extents. In contrast, the (non-significant) negative effects of elevation and drought frequency on the local scale, both variables that vary more strongly between local forest
 340 communities, become more positive on the regional scale. It is also important to consider that EVI, as a proxy for forest productivity, is not necessarily fully coupled with environmental conditions such as drought or seasonality. For instance, some tree species may increase their productivity under drier conditions due to phenology or responses to strong drought events (Janssen et al., 2021), which could potentially weaken the direct link between these environmental drivers and stability metrics.

345 These results highlight that critical slowing down of the Amazon forest is impacted differently by various environmental variables, depending on the spatial scale considered. Most research on the Amazon's response to climate change has focussed either on plot-level studies (Brienen et al., 2015; Esquivel-Muelbert et al., 2019) or coarse-scale satellite time series (Boulton et al., 2022; Van Passel et al., 2024a), often overlooking this scale-dependent aspect of the forest's stability.

4.4 Drivers of gamma stability

350 Consistent with our hypothesis (Fig. 1), our findings indicate that spatial asynchrony exerts a more pronounced positive impact on gamma stability than local stability. This greater relative effect of spatial asynchrony aligns with prior research investigating stability across a large temperate forest ecosystem (Qiao et al., 2022) and can partly be attributed to the high spatial heterogeneity and species turnover characterizing the Amazon forest (Keil & Chase, 2019).

Our results imply that higher alpha and beta diversity exert indirect stabilizing effects on the regional scale by enhancing
 355 alpha stability and spatial asynchrony, respectively. The predominant influence of spatial asynchrony, and thus beta diversity, on gamma stability resonates with studies conducted in temperate forests. These studies similarly highlighted the stronger effects of beta diversity compared to alpha diversity on both ecosystem stability and multifunctionality (Sebal et al., 2021; Van Der Plas et al., 2016). The significance of beta diversity could imply that the high spatial turnover in species composition across the Amazon is closely linked to a high spatial turnover in functional diversity. This, in turn, would lead



360 to local changes in ecosystem functioning that can scale up to large-scale changes in the provision of multiple ecosystem functions, with stability being just one aspect (Mori et al., 2018; Van Der Plas et al., 2016).

4.5 Limitations and perspectives

The tree species richness data used in this study were obtained from published global model predictions rather than direct plot measurements. This approach was necessary due to the absence of spatially comprehensive tree species data covering multiple spatial scales across the Amazon. However, it is important to note that the accuracy of the diversity-stability relationship discussed here is dependent on the accuracy of the diversity predictions. Although the diversity model accounted for more than 90% of the deviance of the data, exhibited low relative uncertainty in the Amazon forest compared to other global biomes, and performed well in the Amazon when validated with external data (Supplementary Fig. 3 in Keil & Chase (2019)), caution should still be exercised in interpreting these results. The significant positive relationship between alpha stability and the globally modelled tree species diversity from Liang et al. (2022) supports our findings, but no significant relationship was found with the Amazon-based estimates from ter Steege et al. (2023) (Fig. A2). Although the former dataset demonstrated greater explanatory power for South America compared to that of ter Steege et al. (2023), this further shows the complexity of understanding the drivers of ecosystem stability in the Amazon forest.

Furthermore, we anticipate that the stabilizing effects of diversity in the Amazon forest across spatial scales would be more pronounced when incorporating functional instead of species diversity metrics. Functional diversity, particularly related to hydraulic traits, has been identified as a crucial factor in explaining the variation of drought responses in tropical forests (Barros et al., 2019). Heterogeneity in the vegetation structure has also been identified as a key driver of stability in temperate forest ecosystems (Qiao et al., 2023), but this heterogeneity is more effectively captured through functional than taxonomic diversity. Prior research has noted a gradual shift of Amazon tree communities towards more dry-affiliated species in response to climate change, although delayed due to the extended generation times of tropical trees (Esquivel-Muelbert et al., 2019). These shifts in compositional dynamics might enhance the stability of the Amazon forest against future droughts, but they could also lead to reduced carbon stocks and other ecosystem functions (Rius et al., 2023), and reduced biodiversity, given the dominance of wet-affiliated tree species among Amazonian trees (Esquivel-Muelbert et al., 2017). Hence, considering the temporal dynamics of diversity would offer valuable insights into the diversity-stability relationship in the Amazon. However, data on tree species and functional diversity within the Amazon remain limited, especially on multiple spatial and temporal scales (Keil & Chase, 2019). Recently, remotely-sensed spectral asynchrony, which captures the spatial heterogeneity of species' functional responses across distinct pixels, has been proposed as a readily monitorable metric for assessing the impacts of species diversity in seasonally dry tropical forests (Mazzochini et al., 2024), offering an alternative to ground-based plant diversity data.

390 Lastly, the use of 20-year EVI-based trends in TAC as a proxy for forest stability has its limitations. Our assumption that the phenology in the Amazon largely explains the remotely sensed EVI patterns was based on previous research (Anderegg et al., 2019; D. Wu et al., 2022; J. Wu et al., 2018). However, because EVI does not capture forest structure, changes in EVI



TAC do not necessarily reflect increased tree mortality but rather shifts in ecosystem functioning. We also restricted our analysis to regions without fires or land-use change, ensuring that differences in disturbance history between pixels were primarily linked to drought occurrences, which we explicitly accounted for. Nonetheless, since both deforestation and degradation can affect tropical forests up to 100 km away (Araujo et al., 2023; Butt et al., 2023), it is unlikely that this masking completely removed their influence. Finally, while the 20-year timescale might be too short to capture long-term stability trends in the Amazon, the inclusion of three widespread drought years within this period enabled us to quantify how diversity influences short-term stability responses.

To gain deeper insights into the complex relationships between diversity and critical slowing down in the Amazon, there is a need for the expansion and integration of more extensive diversity datasets. Nevertheless, our findings highlight the importance of conserving tree species diversity, rather than just forest cover, in maintaining ecosystem stability within the Amazon.

5 Conclusions

By incorporating stability and diversity data across multiple spatial scales, we found more pronounced critical slowing down at the local than regional scale, indicating that Amazonian tipping points are more likely to occur locally than regionally or basin-wide. The weak but significant positive relationships between diversity and stability at both alpha and beta scales highlight both the importance of biodiversity conservation and the complexity of understanding and predicting tropical forest stability. In the face of climate change and more frequent extreme drought occurrences across the Amazon, preserving high tree species diversity at multiple spatial scales could act as a valuable buffer against the Amazon transitioning from a carbon sink to a carbon source.



Appendix A

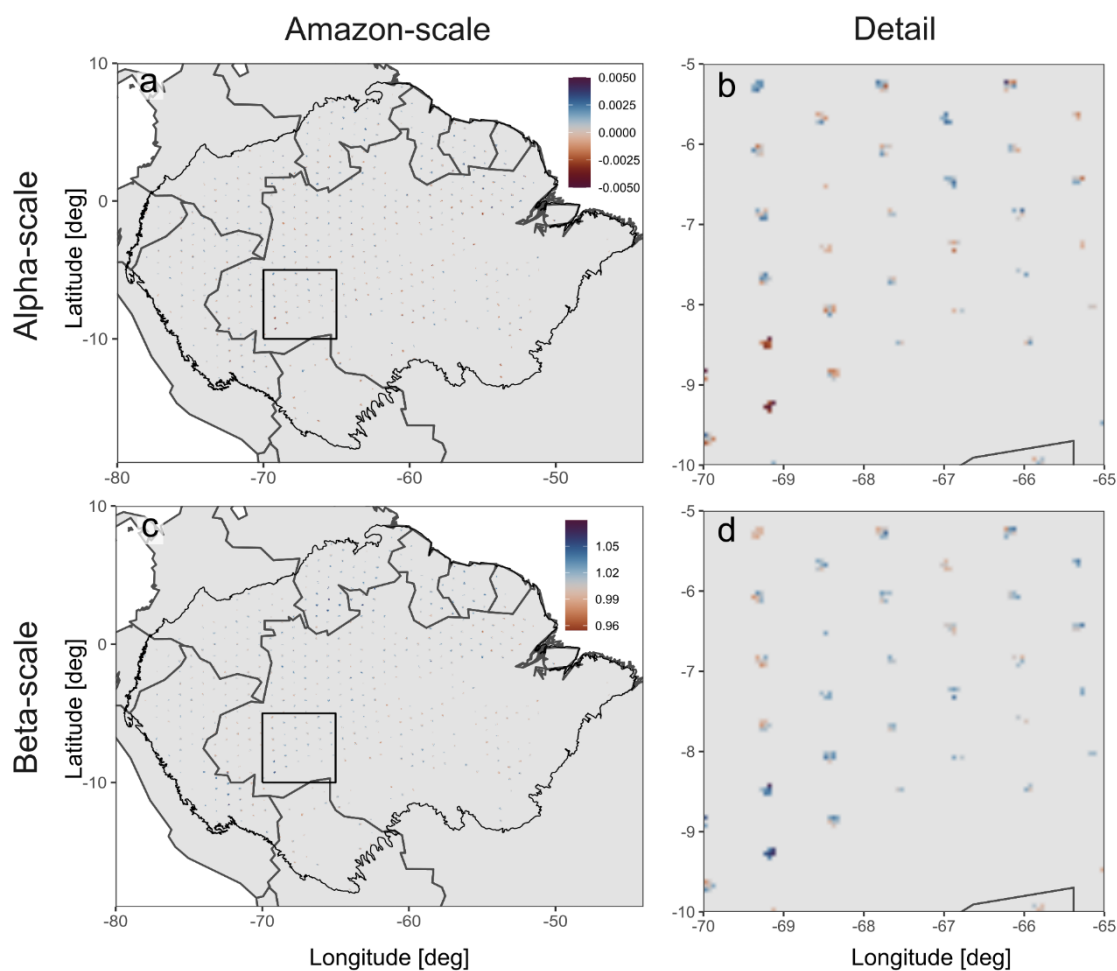
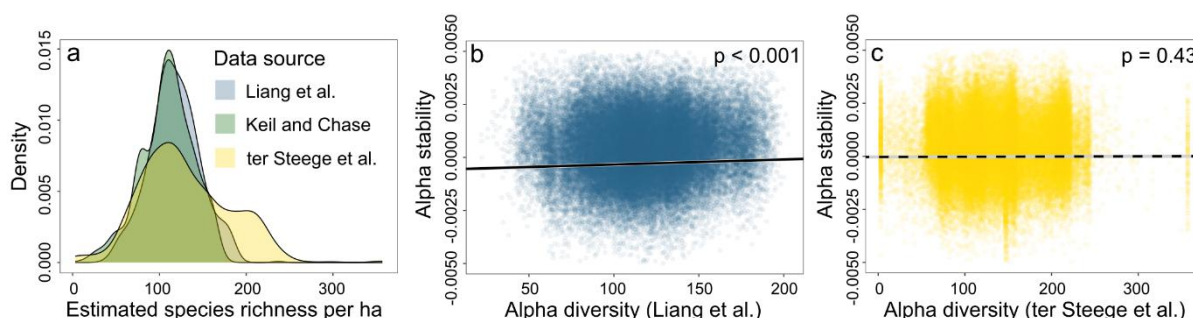


Figure A1: Stability on the alpha and beta scale using the smallest buffer size of 225 km², with the pixels shown at the correct size. (a and b) alpha stability; and (c and d) spatial asynchrony. (b) and (d) show a zoomed-in detail of the Amazon-scale maps.



420 **Figure A2: Comparison with other publicly available tree species richness estimates across the Amazon forest. Liang et al. refers**
 to a globally modelled tree species diversity product with a spatial resolution of 0.025° , based on 1.3 million sample plots (Liang et
 al., 2022). Their model explained 95% of the variance in tree species richness in South America. Ter Steege et al. refers to a
 modelled tree species diversity map of the Amazon with a spatial resolution of 0.1° , based on 2,046 plots (ter Steege et al., 2023).
 425 Their model explained 71% of tree species richness in the Amazon. Keil and Chase refers to the main alpha diversity product used in the manuscript. (a) Density comparison of the different tree species diversity
 estimates in the Amazon. Keil and Chase refers to the main alpha diversity product used in the manuscript. (b) Significant positive
 linear relationship between alpha diversity from Liang et al. (2022) and alpha stability. (c) Non-significant relationship between
 alpha diversity from ter Steege et al. (2023) and alpha stability. (b) and (c) show the marginal effect plots of the models including
 environmental and climatic variables.

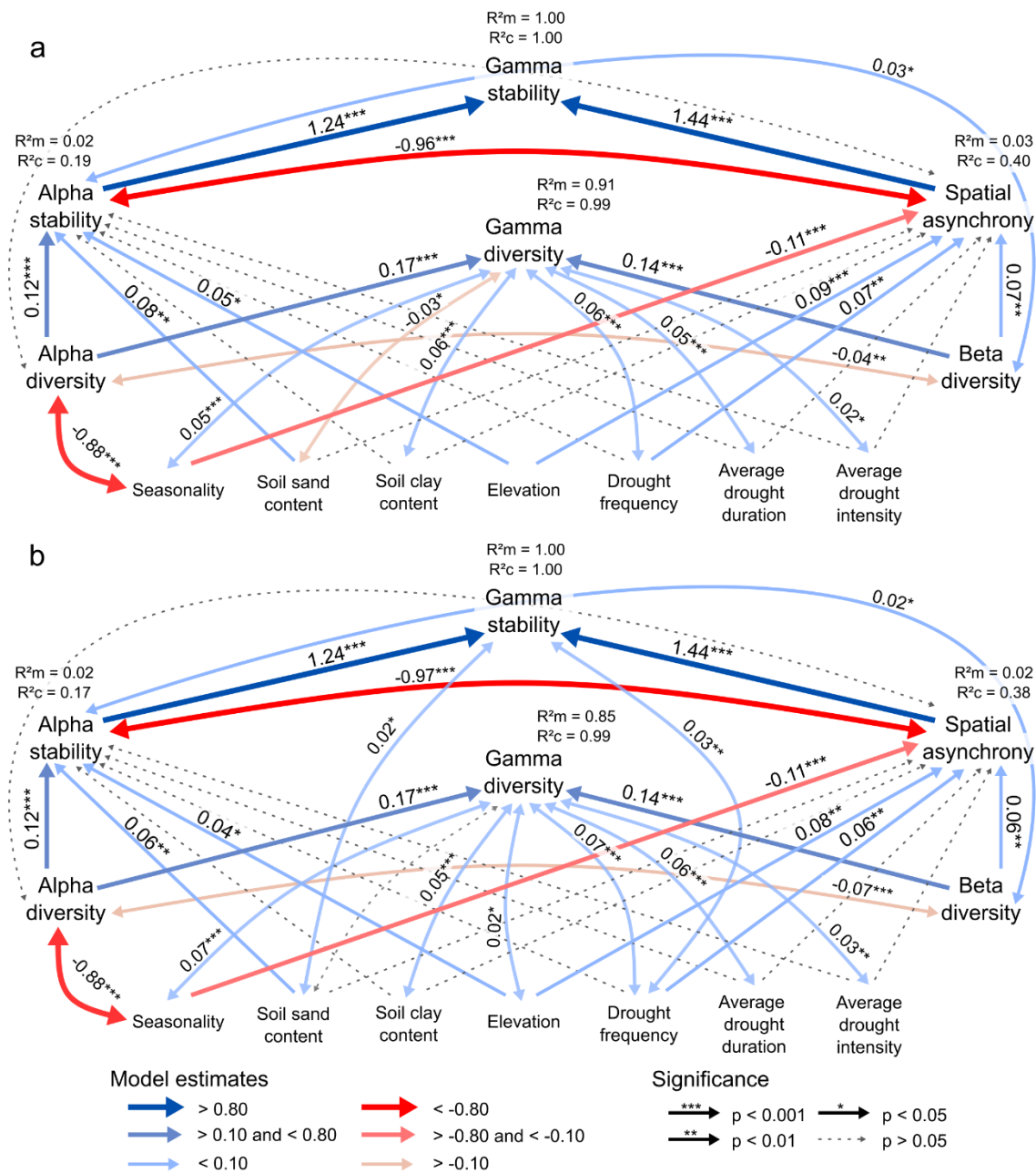
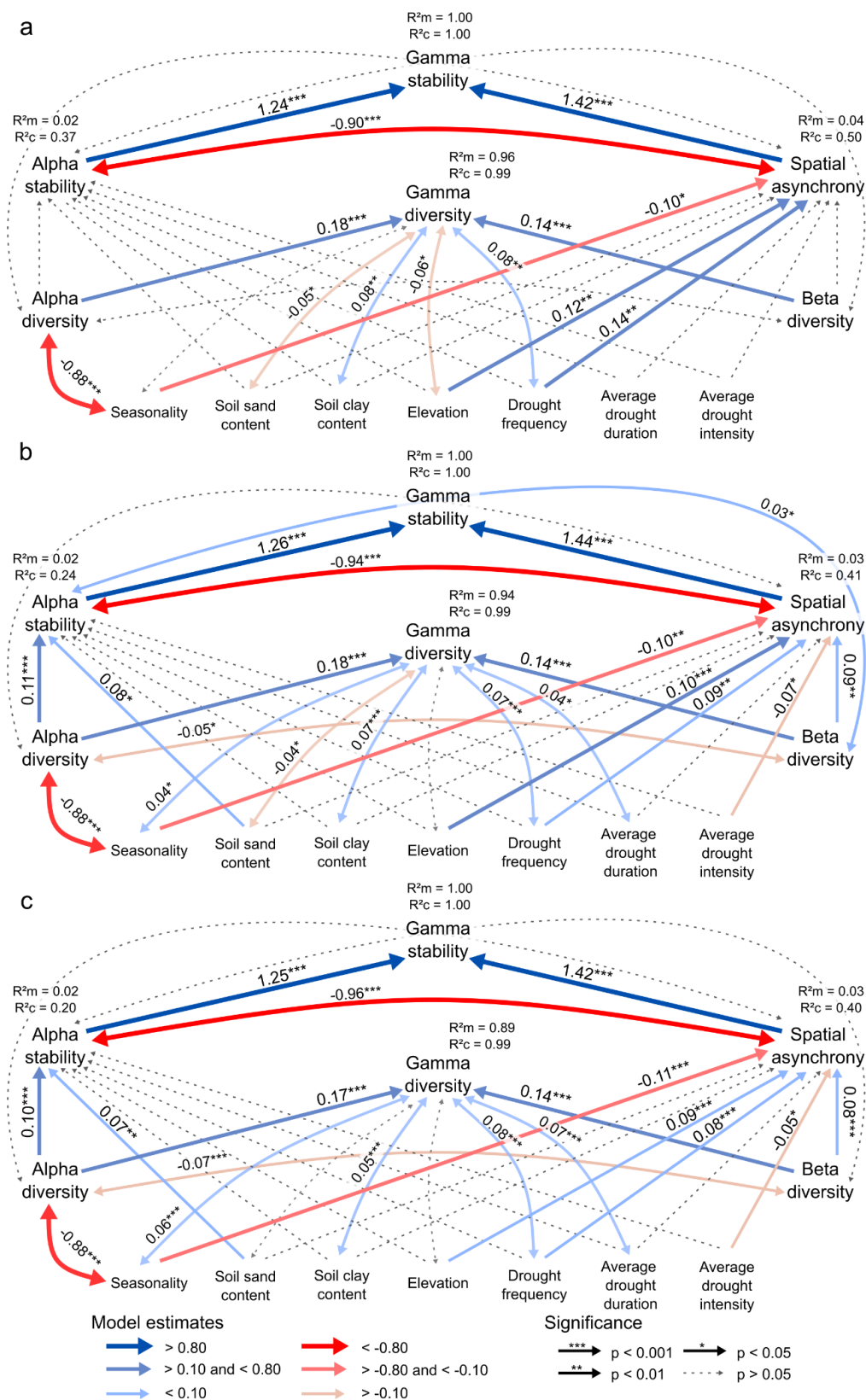


Figure A3: Representation of the structural equation model involving the causal relationships between stability, diversity, environment and drought history across spatial scales, using the trend in TAC calculated as lag-1 autocorrelation, for the buffer sizes of (a) 625 km²; and (b) 1,225 km². (a) Model Fisher's C = 31.1 ($p = 0.15$). (b) Model Fisher's C = 24.8 ($p = 0.21$). The R^2_m and R^2_c values next to the response variables represent the marginal and conditional R^2 values, respectively. The full blue and red arrows indicate significantly positive and negative coefficients ($p < 0.05$), while the dotted lines indicate non-significant effects. The single-headed straight arrows represent causal pathways, and the double-headed curved arrows represent the covarying variables. The numbers on the arrows represent the significant effect sizes of the standardized path coefficients.





440 **Figure A4: Representation of the structural equation model involving the causal relationships between stability, diversity, environment and drought history across spatial scales, using only the 0.05° EVI pixels with a trend in TAC and in SD that do not show significant opposite effects, for the buffer sizes of (a) 225 km², (b) 625 km², and (c) 1,225 km². (a) Model Fisher's C = 36.7 (p = 0.13). (b) Model Fisher's C = 31.4 (p = 0.21). (c) Model Fisher's C = 36.6 (p = 0.08). The R²_m and R²_c values next to the response variables represent the marginal and conditional R² values, respectively. The single-headed straight arrows represent causal pathways, and the double-headed curved arrows represent the covarying variables. The numbers on the arrows represent the significant effect sizes of the standardized path coefficients.**

445

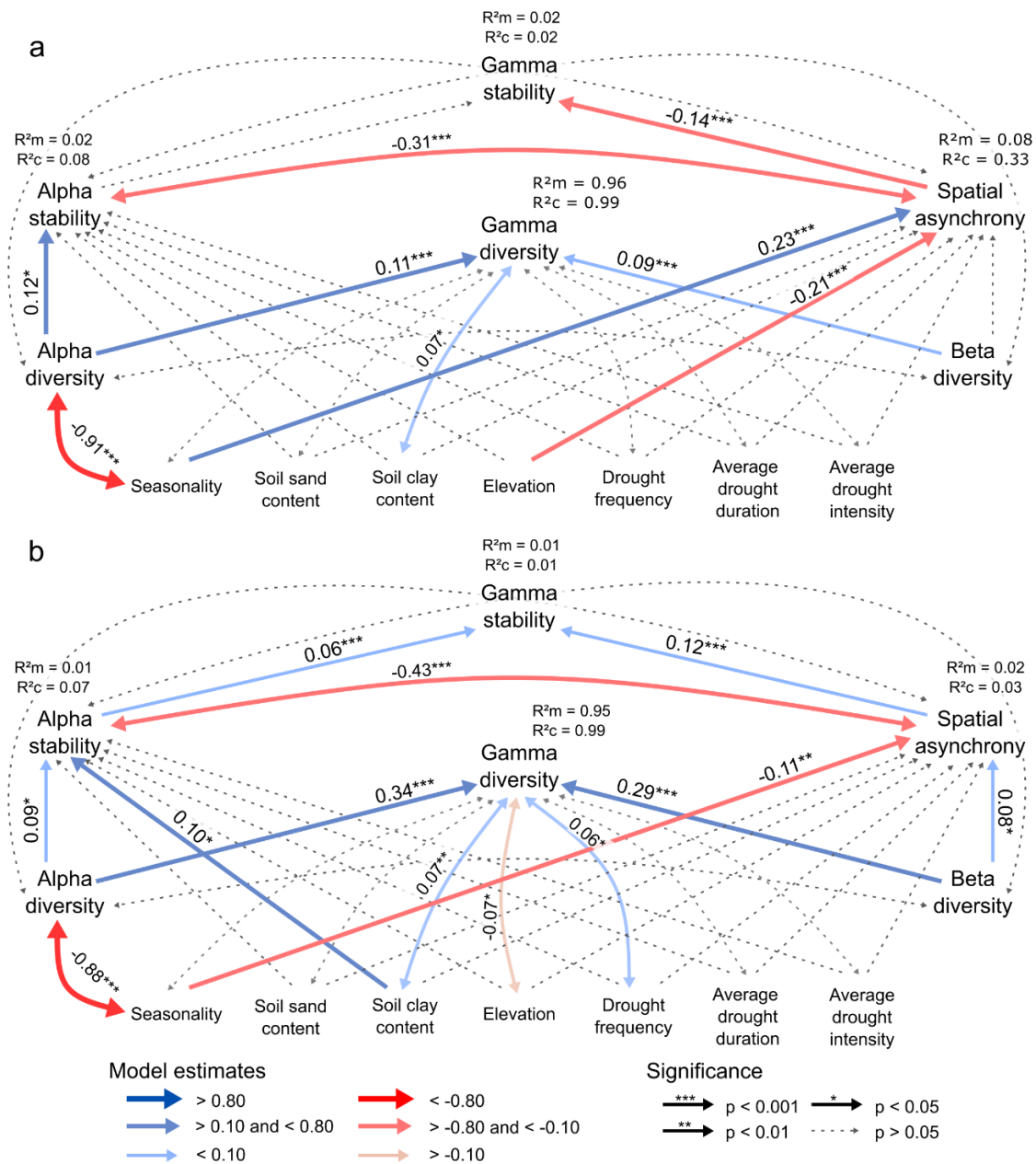


Figure A5: Representation of the structural equation model involving the causal relationships between stability, diversity, environment and drought history across spatial scales, including only (a) negative alpha stability values, and (b) positive alpha stability values. In (a), higher spatial asynchrony values represent a higher regional than local critical slowing down response, which is opposite from the interpretation in the main manuscript, hence the switched signs of some of the relationships. In (b), higher spatial asynchrony values represent a higher local than regional critical slowing down response, similar to the interpretation in the main manuscript. The R^2_m and R^2_c values next to the response variables represent the marginal and conditional R^2 values, respectively. The single-headed straight arrows represent causal pathways, and the double-headed curved arrows represent the covarying variables. The numbers on the arrows represent the significant effect sizes of the standardized path coefficients.

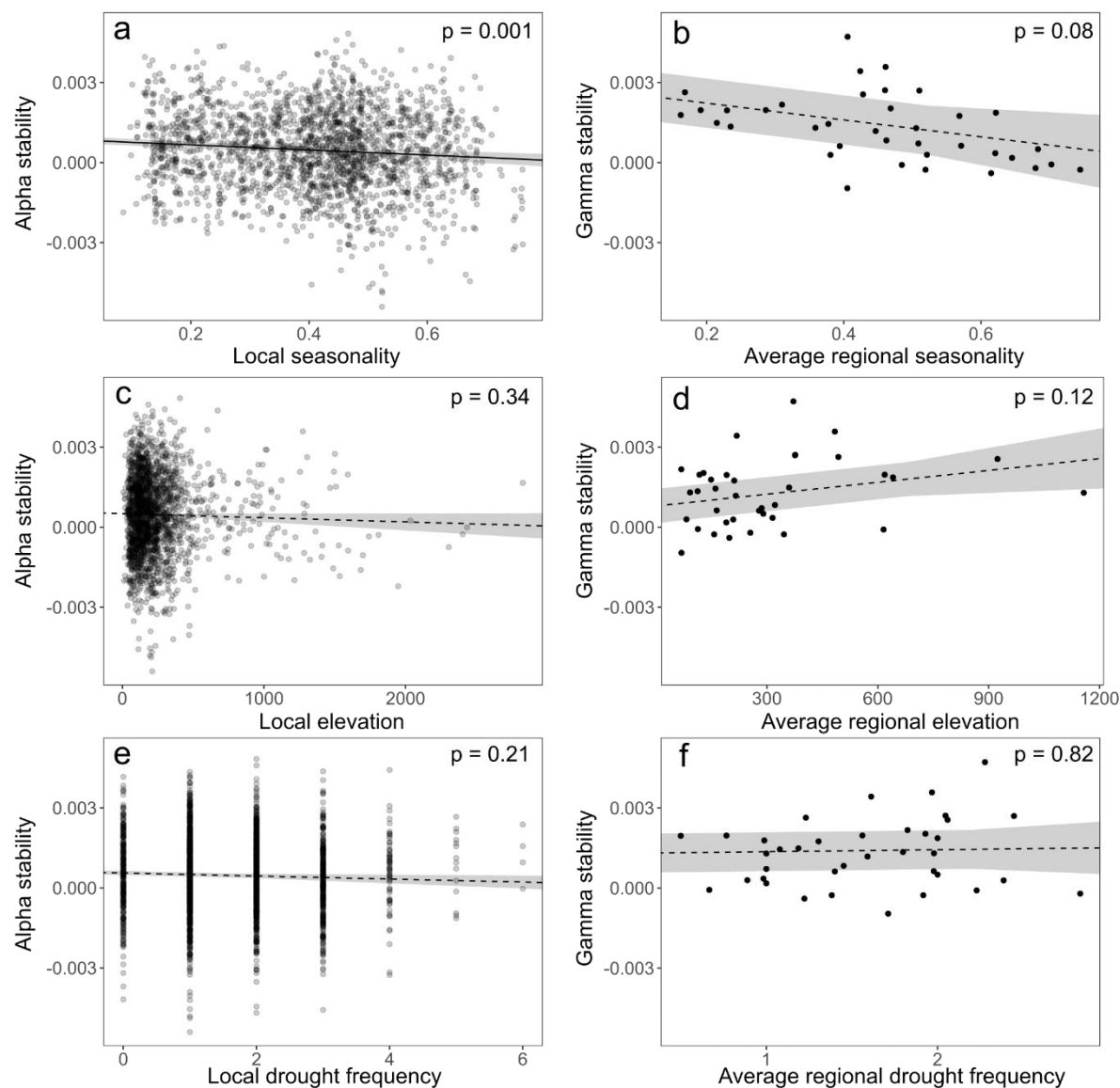


Figure A6: Linear relationships between stability and (a and b) seasonality; (c and d) elevation; and (e and f) drought frequency, on the (a-c-e) alpha and (b-d-f) gamma scale. Spatial autocorrelation was included using an exponential correlation structure in all the models. Dashed and full lines indicate non-significant and significant linear relationships (with $p < 0.05$), respectively. Elevation, seasonality and drought frequency on the gamma scale were calculated as the mean values of all EVI pixels included in the smallest buffer zone of 225 km².



Table A1: Results of the linear diversity-stability relationships on the alpha and beta scale, using the trend in TAC for all EVI pixels, for the three buffer sizes with the 0.05° pixels. R²_m and R²_c are the marginal and conditional R² values, respectively. Significant effect sizes are indicated with asterisks (* p < 0.001; ** p < 0.01; * p < 0.05).**

Buffer radius	size	-	Number of pixels	Number of buffer zones	Alpha effect size	-	Alpha R ² _m – R ² _c	-	Beta effect size	-	Beta R ² _m – R ² _c
225 km ² - 8.5 km			1866	497	6.1 x 10 ⁻⁶ **		0.01 – 0.18		2.0 x 10 ⁻⁴ ***		0.02 – 0.41
625 km ² - 14.1 km			5130	551	6.9 x 10 ⁻⁶ ***		0.01 – 0.19		5.6 x 10 ⁻⁴ ***		0.01 – 0.41
1,225 km ² - 19.7 km			9904	591	6.6 x 10 ⁻⁶ ***		0.01 – 0.17		4.9 x 10 ⁻⁴ ***		0.01 – 0.40

470 **Table A2: Results of the linear diversity-stability relationships on the alpha and beta scale, using only the EVI pixels with a trend in TAC and in SD that do not show significant opposite effects, for the three buffer sizes with the 0.05° pixels. R²_m and R²_c are the marginal and conditional R² values, respectively. Significant effect sizes are indicated with asterisks (*** p < 0.001; ** p < 0.01; * p < 0.05).**

Buffer radius	size	-	Number of pixels	Number of buffer zones	Alpha effect size	-	Alpha R ² _m – R ² _c	-	Beta effect size	-	Beta R ² _m – R ² _c
225 km ² - 8.5 km			1017	434	5.9 x 10 ⁻⁶ *		0.01 – 0.34		7.6 x 10 ⁻⁴ **		0.01 – 0.47
625 km ² - 14.1 km			2761	530	6.9 x 10 ⁻⁶ ***		0.01 – 0.24		7.4 x 10 ⁻⁴ ***		0.01 – 0.41
1,225 km ² - 19.7 km			5400	570	5.9 x 10 ⁻⁶ ***		0.01 – 0.20		6.4 x 10 ⁻⁴ ***		0.01 – 0.40

Code availability

475 The R scripts used for the analyses in this research can be found on the private figshare repository: <https://figshare.com/s/dfa69fb1b9a30b9ebcdc>, which will be published with the publication of the manuscript.

Data availability

The alpha stability data used in this research is stored in a published figshare repository (Van Passel et al., 2024b): <https://figshare.com/s/0363ff12d5bee640524b>. The diversity data is freely available from Keil & Chase (2019).



480 **Author contributions**

J.V.P., W.D.K., K.V.M., and B.S. contributed to the design of the research. J.V.P. performed the analyses. All authors contributed to the interpretation of the results and the writing of the manuscript.

Competing interests

The authors declare that they have no conflict of interest.

485 **Acknowledgements**

We used the assistance of the Large Language Model, ChatGPT, to improve the fluency and readability of the text.

Financial support

JVP received funding from the Research Foundation Flanders (FWO) (grant number G063420N and 12A2L25N). PNB received funding from the Research Foundation Flanders (FWO) (grant number G0F6922N). This work was supported by
490 the Serrapilheira Institute (grant number Serra-1709-18983).

References

- Abatzoglou, J. T., Dobrowski, S. Z., Parks, S. A., & Hegewisch, K. C. (2018). TerraClimate, a high-resolution global dataset of monthly climate and climatic water balance from 1958-2015. *Scientific Data*, 5, 1–12. <https://doi.org/10.1038/sdata.2017.191>
- 495 Anderegg, W. R. L., Anderegg, L. D. L., & Huang, C. (2019). Testing early warning metrics for drought-induced tree physiological stress and mortality. *Global Change Biology*, 25(7), 2459–2469. <https://doi.org/10.1111/gcb.14655>
- Aragão, L. E. O. C., Malhi, Y., Roman-Cuesta, R. M., Saatchi, S., Anderson, L. O., & Shimabukuro, Y. E. (2007). Spatial patterns and fire response of recent Amazonian droughts. *Geophysical Research Letters*, 34(7), 1–5. <https://doi.org/10.1029/2006GL028946>
- 500 Araujo, R., Assunção, J., Hirota, M., & Scheinkman, J. A. (2023). Estimating the spatial amplification of damage caused by degradation in the Amazon. *Proceedings of the National Academy of Sciences*, 120(46), e2312451120. <https://doi.org/10.1073/pnas.2312451120>
- Artaxo, P. (2023). Amazon deforestation implications in local/regional climate change. *Proceedings of the National Academy of Sciences*, 120(50), e2317456120. <https://doi.org/10.1073/pnas.2317456120>



- 505 Barros, F. de V., Bittencourt, P. R. L., Brum, M., Restrepo-Coupe, N., Pereira, L., Teodoro, G. S., Saleska, S. R., Borma, L. S., Christoffersen, B. O., Penha, D., Alves, L. F., Lima, A. J. N., Carneiro, V. M. C., Gentine, P., Lee, J., Aragão, L. E. O. C., Ivanov, V., Leal, L. S. M., Araujo, A. C., & Oliveira, R. S. (2019). Hydraulic traits explain differential responses of Amazonian forests to the 2015 El Niño-induced drought. *New Phytologist*, 223(3), 1253–1266. <https://doi.org/10.1111/nph.15909>
- 510 Bennett, A. C., Rodrigues De Sousa, T., Monteagudo-Mendoza, A., Esquivel-Muelbert, A., Morandi, P. S., Coelho De Souza, F., Castro, W., Duque, L. F., Flores Llampaço, G., Manoel Dos Santos, R., Ramos, E., Vilanova Torre, E., Alvarez-Davila, E., Baker, T. R., Costa, F. R. C., Lewis, S. L., Marimon, B. S., Schietti, J., Burban, B., ... Phillips, O. L. (2023). Sensitivity of South American tropical forests to an extreme climate anomaly. *Nature Climate Change*, 13(9), 967–974. <https://doi.org/10.1038/s41558-023-01776-4>
- 515 Boulton, C. A., Lenton, T. M., & Boers, N. (2022). Pronounced loss of Amazon rainforest resilience since the early 2000s. *Nature Climate Change*, 12(3), 271–278. <https://doi.org/10.1038/s41558-022-01287-8>
Brienen, R. J. W., Phillips, O. L., Feldpausch, T. R., Gloor, E., Baker, T. R., Lloyd, J., Lopez-Gonzalez, G., Monteagudo-Mendoza, A., Malhi, Y., Lewis, S. L., Vásquez Martínez, R., Alexiades, M., Álvarez Dávila, E., Alvarez-Loayza, P., Andrade, A., Aragão, L. E. O. C., Araujo-Murakami, A., Arets, E. J. M. M., Arroyo, L., ... Zagt, R. J. (2015). Long-term
520 decline of the Amazon carbon sink. *Nature*, 519(7543), 344–348. <https://doi.org/10.1038/nature14283>
Buckley, L. B., & Jetz, W. (2008). Linking global turnover of species and environments. *Proceedings of the National Academy of Sciences*, 105(46), 17836–17841. <https://doi.org/10.1073/pnas.0803524105>
Butt, E. W., Baker, J. C. A., Bezerra, F. G. S., Von Randow, C., Aguiar, A. P. D., & Spracklen, D. V. (2023). Amazon deforestation causes strong regional warming. *Proceedings of the National Academy of Sciences*, 120(45), e2309123120.
525 <https://doi.org/10.1073/pnas.2309123120>
Cleveland, R. B., Cleveland, W. S., McRae, J. E., & Terpenning, I. (1990). STL: A Seasonal-Trend Decomposition Procedure Based on Loess. *Journal of Official Statistics*, 6(1), 3–73.
Costa, F. R. C., Schietti, J., Stark, S. C., & Smith, M. N. (2023). The other side of tropical forest drought: Do shallow water table regions of Amazonia act as large-scale hydrological refugia from drought? *New Phytologist*, 237(3), 714–733.
530 <https://doi.org/10.1111/nph.17914>
Dakos, V., Carpenter, S. R., Brock, W. A., Ellison, A. M., Guttal, V., Ives, A. R., Kéfi, S., Livina, V., Seekell, D. A., van Nes, E. H., & Scheffer, M. (2012). Methods for detecting early warnings of critical transitions in time series illustrated using simulated ecological data. *PLoS ONE*, 7(7). <https://doi.org/10.1371/journal.pone.0041010>
Dakos, V., & Kéfi, S. (2022). Ecological resilience: What to measure and how. *Environmental Research Letters*, 17(4), 043003. <https://doi.org/10.1088/1748-9326/ac5767>
535 DiMiceli, C., Carroll, M., Sohlberg, R., Kim, D., Kelly, M., & Townshend, J. (2015). MOD44B MODIS/Terra Vegetation Continuous Fields Yearly L3 Global 250m SIN Grid V006 [Data set]. NASA EOSDIS Land Processes DAAC. <https://doi.org/10.5067/MODIS/MOD44B.006>



- Ditlevsen, P. D., & Johnsen, S. J. (2010). Tipping points: Early warning and wishful thinking. *Geophysical Research Letters*, 37(19), n/a-n/a. <https://doi.org/10.1029/2010GL044486>
- Esquivel-Muelbert, A., Baker, T. R., Dexter, K. G., Lewis, S. L., Brien, R. J. W., Feldpausch, T. R., Lloyd, J., Monteagudo-Mendoza, A., Arroyo, L., Álvarez-Dávila, E., Higuchi, N., Marimon, B. S., Marimon-Junior, B. H., Silveira, M., Vilanova, E., Gloor, E., Malhi, Y., Chave, J., Barlow, J., ... Phillips, O. L. (2019). Compositional response of Amazon forests to climate change. *Global Change Biology*, 25(1), 39–56. <https://doi.org/10.1111/gcb.14413>
- Esquivel-Muelbert, A., Baker, T. R., Dexter, K. G., Lewis, S. L., ter Steege, H., Lopez-Gonzalez, G., Monteagudo Mendoza, A., Brien, R., Feldpausch, T. R., Pitman, N., Alonso, A., van der Heijden, G., Peña-Claros, M., Ahuite, M., Alexiades, M., Álvarez Dávila, E., Murakami, A. A., Arroyo, L., Aulestia, M., ... Phillips, O. L. (2017). Seasonal drought limits tree species across the Neotropics. *Ecography*, 40(5), 618–629. <https://doi.org/10.1111/ecog.01904>
- Flores, B. M., Montoya, E., Sakschewski, B., Nascimento, N., Staal, A., Betts, R. A., Levis, C., Lapola, D. M., Esquivel-Muelbert, A., Jakovac, C., Nobre, C. A., Oliveira, R. S., Borma, L. S., Nian, D., Boers, N., Hecht, S. B., Ter Steege, H., Arieira, J., Lucas, I. L., ... Hirota, M. (2024). Critical transitions in the Amazon forest system. *Nature*, 626(7999), 555–564. <https://doi.org/10.1038/s41586-023-06970-0>
- Giglio, L., Justice, C., Boschetti, L., & Roy, D. (2015). MCD64A1 MODIS/Terra+Aqua Burned Area Monthly L3 Global 500m SIN Grid V006 [Data set]. NASA EOSDIS Land Processes DAAC. <https://doi.org/10.5067/MODIS/MCD64A1.006>
- Gomes, V. H. F., Vieira, I. C. G., Salomão, R. P., & Ter Steege, H. (2019). Amazonian tree species threatened by deforestation and climate change. *Nature Climate Change*, 9(7), 547–553. <https://doi.org/10.1038/s41558-019-0500-2>
- Gonzalez, A., Germain, R. M., Srivastava, D. S., Filotas, E., Dee, L. E., Gravel, D., Thompson, P. L., Isbell, F., Wang, S., Kéfi, S., Montoya, J., Zelnik, Y. R., & Loreau, M. (2020). Scaling-up biodiversity-ecosystem functioning research. *Ecology Letters*, 23(4), 757–776. <https://doi.org/10.1111/ele.13456>
- Grossiord, C., Granier, A., Rateliffé, S., Bouriaud, O., Bruelheide, H., Chećko, E., Forrester, D. I., Dawud, S. M., Finér, L., Pollastrini, M., Scherer-Lorenzen, M., Valladares, F., Bonal, D., & Gessler, A. (2014). Tree diversity does not always improve resistance of forest ecosystems to drought. *Proceedings of the National Academy of Sciences*, 111(41), 14812–14815. <https://doi.org/10.1073/pnas.1411970111>
- Hautier, Y., Zhang, P., Loreau, M., Wilcox, K. R., Seabloom, E. W., Borer, E. T., Byrnes, J. E. K., Koerner, S. E., Komatsu, K. J., Lefcheck, J. S., Hector, A., Adler, P. B., Alberti, J., Arnillas, C. A., Bakker, J. D., Brudvig, L. A., Bugalho, M. N., Cadotte, M., Caldeira, M. C., ... Wang, S. (2020). General destabilizing effects of eutrophication on grassland productivity at multiple spatial scales. *Nature Communications*, 11(1), 5375. <https://doi.org/10.1038/s41467-020-19252-4>
- Hoorn, C., Wesselingh, F. P., Ter Steege, H., Bermudez, M. A., Mora, A., Sevink, J., Sanmartín, I., Sanchez-Meseguer, A., Anderson, C. L., Figueiredo, J. P., Jaramillo, C., Riff, D., Negri, F. R., Hooghiemstra, H., Lundberg, J., Stadler, T., Särkinen, T., & Antonelli, A. (2010). Amazonia Through Time: Andean Uplift, Climate Change, Landscape Evolution, and Biodiversity. *Science*, 330(6006), 927–931. <https://doi.org/10.1126/science.1194585>



- Hutchison, C., Gravel, D., Guichard, F., & Potvin, C. (2018). Effect of diversity on growth, mortality, and loss of resilience to extreme climate events in a tropical planted forest experiment. *Scientific Reports*, 8(1), 15443. <https://doi.org/10.1038/s41598-018-33670-x>
- 575 IPCC. (2021). Summary for Policymakers. In V. Masson-Delmotte, P. Zhai, A. Pirani, S. L. Connors, C. Péan, S. Berger, N. Caud, Y. Chen, L. Goldfarb, M. I. Gomis, M. Huang, K. Leitzell, E. Lonnoy, J. B. R. Matthews, T. K. Maycock, T. Waterfield, O. Yelekçi, R. Yu, & B. Zhou (Eds.), *Climate Change 2021: The Physical Science Basis. Contribution of Working Group I to the Sixth Assessment Report of the Intergovernmental Panel on Climate Change* (p. 42). Cambridge University Press (In press).
- 580 Isbell, F., Craven, D., Connolly, J., Loreau, M., Schmid, B., Beierkuhnlein, C., Bezemer, T. M., Bonin, C., Bruehlheide, H., de Luca, E., Ebeling, A., Griffin, J. N., Guo, Q., Hautier, Y., Hector, A., Jentsch, A., Kreyling, J., Lanta, V., Manning, P., ... Eisenhauer, N. (2015). Biodiversity increases the resistance of ecosystem productivity to climate extremes. *Nature*, 526(7574), 574–577. <https://doi.org/10.1038/nature15374>
- Ismaeel, A., Tai, A. P. K., Santos, E. G., Maraia, H., Aalto, I., Altman, J., Doležal, J., Lembrechts, J. J., Camargo, J. L.,
 585 Aalto, J., Sam, K., Avelino Do Nascimento, L. C., Kopecký, M., Svátek, M., Nunes, M. H., Matula, R., Plichta, R., Abera, T., & Maeda, E. E. (2024). Patterns of tropical forest understory temperatures. *Nature Communications*, 15(1), 549. <https://doi.org/10.1038/s41467-024-44734-0>
- Janssen, T., Fleischer, K., Luyssaert, S., Naudts, K., & Dolman, H. (2020). Drought resistance increases from the individual to the ecosystem level in highly diverse Neotropical rainforest: A meta-analysis of leaf, tree and ecosystem responses to
 590 drought. *Biogeosciences*, 17(9), 2621–2645. <https://doi.org/10.5194/bg-17-2621-2020>
- Janssen, T., Van Der Velde, Y., Hofhansl, F., Luyssaert, S., Naudts, K., Driessen, B., Fleischer, K., & Dolman, H. (2021). Drought effects on leaf fall, leaf flushing and stem growth in the Amazon forest: Reconciling remote sensing data and field observations. *Biogeosciences*, 18(14), 4445–4472. <https://doi.org/10.5194/bg-18-4445-2021>
- Keil, P., & Chase, J. M. (2019). Global patterns and drivers of tree diversity integrated across a continuum of spatial grains.
 595 *Nature Ecology & Evolution*, 3(3), 390–399. <https://doi.org/10.1038/s41559-019-0799-0>
- Laurance, W. F., Fearnside, P. M., Laurance, S. G., Delamonica, P., Lovejoy, T. E., Rankin-de Merona, J. M., Chambers, J. Q., & Gascon, C. (1999). Relationship between soils and Amazon forest biomass: A landscape-scale study. *Forest Ecology and Management*, 118(1–3), 127–138. [https://doi.org/10.1016/S0378-1127\(98\)00494-0](https://doi.org/10.1016/S0378-1127(98)00494-0)
- Lefcheck, J. S. (2016). *piecewiseSEM: Piecewise structural equation modelling in r for ecology, evolution, and systematics*.
 600 *Methods in Ecology and Evolution*, 7, 573–579. <https://doi.org/10.1111/2041-210X.12512>
- Lenton, T. M., Buxton, J. E., Armstrong McKay, D. I., Abrams, J. F., Boulton, C. A., Lees, K., Powell, T. W. R., Boers, N., Cunliffe, A. M., & Dakos, V. (2022). A resilience sensing system for the biosphere. *Philosophical Transactions of the Royal Society B: Biological Sciences*, 377(1857), 20210383. <https://doi.org/10.1098/rstb.2021.0383>
- Levis, C., Costa, F. R. C., Bongers, F., Peña-Claros, M., Clement, C. R., Junqueira, A. B., Neves, E. G., Tamanaha, E. K.,
 605 Figueiredo, F. O. G., Salomão, R. P., Castilho, C. V., Magnusson, W. E., Phillips, O. L., Guevara, J. E., Sabatier, D., Molino,



- J.-F., López, D. C., Mendoza, A. M., Pitman, N. C. A., ... Ter Steege, H. (2017). Persistent effects of pre-Columbian plant domestication on Amazonian forest composition. *Science*, 355(6328), 925–931. <https://doi.org/10.1126/science.aal0157>
- Liang, J., Gamarra, J. G. P., Picard, N., Zhou, M., Pijanowski, B., Jacobs, D. F., Reich, P. B., Crowther, T. W., Nabuurs, G.-J., de-Miguel, S., Fang, J., Woodall, C. W., Svenning, J.-C., Jucker, T., Bastin, J.-F., Wiser, S. K., Slik, F., Hérault, B., Alberti, G., ... Hui, C. (2022). Co-limitation towards lower latitudes shapes global forest diversity gradients. *Nature Ecology & Evolution*, 6(10), 1423–1437. <https://doi.org/10.1038/s41559-022-01831-x>
- Liang, M., Baiser, B., Hallett, L. M., Hautier, Y., Jiang, L., Loreau, M., Record, S., Sokol, E. R., Zarnetske, P. L., & Wang, S. (2022). Consistent stabilizing effects of plant diversity across spatial scales and climatic gradients. *Nature Ecology & Evolution*, 6(11), 1669–1675. <https://doi.org/10.1038/s41559-022-01868-y>
- Liu, D., Wang, T., Peñuelas, J., & Piao, S. (2022). Drought resistance enhanced by tree species diversity in global forests. *Nature Geoscience*, 15(10), 800–804. <https://doi.org/10.1038/s41561-022-01026-w>
- Luize, B. G., Tuomisto, H., Ekelschot, R., Dexter, K. G., Amaral, I. L. D., Coelho, L. D. S., Matos, F. D. D. A., Lima Filho, D. D. A., Salomão, R. P., Wittmann, F., Castilho, C. V., Carim, M. D. J. V., Guevara, J. E., Phillips, O. L., Magnusson, W. E., Sabatier, D., Cardenas Revilla, J. D., Molino, J.-F., Ireme, M. V., ... Ter Steege, H. (2024). The biogeography of the Amazonian tree flora. *Communications Biology*, 7(1), 1240. <https://doi.org/10.1038/s42003-024-06937-5>
- Mattos, C. R. C., Mazzochini, G. G., Rius, B. F., Penha, D., Giacomini, L. L., Flores, B. M., Silva, M. C., Xavier, R. O., Nehemy, M. F., Petroni, A. R., Silva, J. S. G. M., Schlickmann, M. B., Rocha, M., Rodrigues, G., Costa, S. S., Barros, F. V., Tavares, J. V., Furtado, M. N., Verona, L. S., ... Hirota, M. (2023). Rainfall and topographic position determine tree embolism resistance in Amazônia and Cerrado sites. *Environmental Research Letters*, 18(11), 114009. <https://doi.org/10.1088/1748-9326/ad0064>
- Mazzochini, G. G., Rowland, L., Lira-Martins, D., Barros, F. D. V., Flores, B. M., Hirota, M., Pennington, R. T., & Oliveira, R. S. (2024). Spectral asynchrony as a measure of ecosystem response diversity. *Global Change Biology*, 30(2), e17174. <https://doi.org/10.1111/gcb.17174>
- Mori, A. S., Isbell, F., & Seidl, R. (2018). β -Diversity, Community Assembly, and Ecosystem Functioning. *Trends in Ecology & Evolution*, 33(7), 549–564. <https://doi.org/10.1016/j.tree.2018.04.012>
- NASA JPL. (2013). NASA Shuttle Radar Topography Mission Global 3 arc second [Data set]. NASA EOSDIS Land Processes DAAC. <https://doi.org/10.5067/MEaSUREs/SRTM/SRTMGL3.003>
- Oliveira, R. S., Eller, C. B., Barros, F. de V., Hirota, M., Brum, M., & Bittencourt, P. (2021). Linking plant hydraulics and the fast–slow continuum to understand resilience to drought in tropical ecosystems. In *New Phytologist* (Vol. 230, Issue 3). <https://doi.org/10.1111/nph.17266>
- Olson, D. M., Dinerstein, E., Wikramanayake, E. D., Burgess, N. D., Powell, G. V. N., Underwood, E. C., & Kassem, K. R. (2001). Terrestrial Ecoregions of the World: A New Map of Life on Earth. *Bioscience*, 51(11), 933–938. [https://doi.org/10.1641/0006-3568\(2001\)051%5B0933:TEOTWA%5D2.0.CO;2](https://doi.org/10.1641/0006-3568(2001)051%5B0933:TEOTWA%5D2.0.CO;2)



- Ouyang, S., Xiang, W., Gou, M., Chen, L., Lei, P., Xiao, W., Deng, X., Zeng, L., Li, J., Zhang, T., Peng, C., & Forrester, D. I. (2021). Stability in subtropical forests: The role of tree species diversity, stand structure, environmental and socio-economic conditions. *Global Ecology and Biogeography*, 30(2), 500–513. <https://doi.org/10.1111/geb.13235>
- Pinheiro, J., Bates, D., DebRoy, S., Sarkar, D., & R Core Team. (2021). nlme: Linear and Nonlinear Mixed Effects Models [Computer software]. <https://cran.r-project.org/package=nlme>
- Poggio, L., De Sousa, L. M., Batjes, N. H., Heuvelink, G. B. M., Kempen, B., Ribeiro, E., & Rossiter, D. (2021). SoilGrids 2.0: Producing soil information for the globe with quantified spatial uncertainty. *Soil*, 7(1), 217–240. <https://doi.org/10.5194/soil-7-217-2021>
- Poorter, L., van der Sande, M. T., Thompson, J., Arets, E. J. M. M., Alarcón, A., Álvarez-Sánchez, J., Ascarrunz, N., Balvanera, P., Barajas-Guzmán, G., Boit, A., Bongers, F., Carvalho, F. A., Casanoves, F., Cornejo-Tenorio, G., Costa, F. R. C., de Castilho, C. V., Duivenvoorden, J. F., Dutrieux, L. P., Enquist, B. J., ... Peña-Claros, M. (2015). Diversity enhances carbon storage in tropical forests. *Global Ecology and Biogeography*, 24(11), 1314–1328. <https://doi.org/10.1111/geb.12364>
- Potapov, P., Yaroshenko, A., Turubanova, S., Dubinin, M., Laestadius, L., Thies, C., Aksenov, D., Egorov, A., Yesipova, Y., Glushkov, I., Karpachevskiy, M., Kostikova, A., Manisha, A., Tsybikova, E., & Zhuravleva, I. (2008). Mapping the World's Intact Forest Landscapes by Remote Sensing. *Ecology and Society*, 13(2).
- Qiao, X., Geng, Y., Zhang, C., Han, Z., Zhang, Z., Zhao, X., von Gadow, K., & Simova, I. (2022). Spatial asynchrony matters more than alpha stability in stabilizing ecosystem productivity in a large temperate forest region. *Global Ecology and Biogeography*, 31(6), 1133–1146. <https://doi.org/10.1111/geb.13488>
- Qiao, X., Hautier, Y., Geng, Y., Wang, S., Wang, J., Zhang, N., Zhang, Z., Zhang, C., Zhao, X., & von Gadow, K. (2023). Biodiversity contributes to stabilizing ecosystem productivity across spatial scales as much as environmental heterogeneity in a large temperate forest region. *Forest Ecology and Management*, 529, 120695. <https://doi.org/10.1016/j.foreco.2022.120695>
- R Core Team. (2024). R: A language and environment for statistical computing [Computer software]. R Foundation for Statistical Computing. <https://www.r-project.org/>
- Rius, B. F., Filho, J. P. D., Fleischer, K., Hofhansl, F., Blanco, C. C., Rammig, A., Domingues, T. F., & Lapola, D. M. (2023). Higher functional diversity improves modeling of Amazon forest carbon storage. *Ecological Modelling*, 481, 110323. <https://doi.org/10.1016/j.ecolmodel.2023.110323>
- Schaaf, C., & Wang, Z. (2015). MCD43C4 MODIS/Terra+Aqua BRDF/Albedo Nadir BRDF-Adjusted Ref Daily L3 Global 0.05Deg CMG V006 [Data set]. NASA EOSDIS Land Processes DAAC. <https://doi.org/10.5067/MODIS/MCD43C4.006>
- Scheffer, M., Bascompte, J., Brock, W. A., Brovkin, V., Carpenter, S. R., Dakos, V., Held, H., Van Nes, E. H., Rietkerk, M., & Sugihara, G. (2009). Early-warning signals for critical transitions. *Nature*, 461(7260), 53–59. <https://doi.org/10.1038/nature08227>



- Sebald, J., Thrippleton, T., Rammer, W., Bugmann, H., & Seidl, R. (2021). Mixing tree species at different spatial scales: The effect of alpha, beta and gamma diversity on disturbance impacts under climate change. *Journal of Applied Ecology*, 58(8), 1749–1763. <https://doi.org/10.1111/1365-2664.13912>
- 675 ter Steege, H., Pitman, N. C. A., Do Amaral, I. L., De Souza Coelho, L., De Almeida Matos, F. D., De Andrade Lima Filho, D., Salomão, R. P., Wittmann, F., Castilho, C. V., Guevara, J. E., Veiga Carim, M. D. J., Phillips, O. L., Magnusson, W. E., Sabatier, D., Revilla, J. D. C., Molino, J.-F., Irumé, M. V., Martins, M. P., Da Silva Guimarães, J. R., ... Melgão, K. (2023). Mapping density, diversity and species-richness of the Amazon tree flora. *Communications Biology*, 6(1), 1130. <https://doi.org/10.1038/s42003-023-05514-6>
- 680 ter Steege, H., Pitman, N. C. A., Phillips, O. L., Chave, J., Sabatier, D., Duque, A., Molino, J.-F., Prévost, M.-F., Spichiger, R., Castellanos, H., Von Hildebrand, P., & Vásquez, R. (2006). Continental-scale patterns of canopy tree composition and function across Amazonia. *Nature*, 443(7110), 444–447. <https://doi.org/10.1038/nature05134>
- ter Steege, H., Prado, P. I., Lima, R. A. F. de, Pos, E., de Souza Coelho, L., de Andrade Lima Filho, D., Salomão, R. P., Amaral, I. L., de Almeida Matos, F. D., Castilho, C. V., Phillips, O. L., Guevara, J. E., de Jesus Veiga Carim, M., Cárdenas López, D., Magnusson, W. E., Wittmann, F., Martins, M. P., Sabatier, D., Irumé, M. V., ... Pickavance, G. (2020). Biased-
 685 corrected richness estimates for the Amazonian tree flora. *Scientific Reports*, 10(1), 1–13. <https://doi.org/10.1038/s41598-020-66686-3>
- Tuomisto, H., Van Doninck, J., Ruokolainen, K., Moulatlet, G. M., Figueiredo, F. O. G., Sirén, A., Cárdenas, G., Lehtonen, S., & Zuquim, G. (2019). Discovering floristic and geoeological gradients across Amazonia. *Journal of Biogeography*, 46(8), 1734–1748. <https://doi.org/10.1111/jbi.13627>
- 690 Van Der Plas, F., Hennecke, J., Chase, J. M., Van Ruijven, J., & Barry, K. E. (2023). Universal beta-diversity–functioning relationships are neither observed nor expected. *Trends in Ecology & Evolution*, 38(6), 532–544. <https://doi.org/10.1016/j.tree.2023.01.008>
- Van Der Plas, F., Manning, P., Soliveres, S., Allan, E., Scherer-Lorenzen, M., Verheyen, K., Wirth, C., Zavala, M. A., Ampoorter, E., Baeten, L., Barbaro, L., Bauhus, J., Benavides, R., Benneter, A., Bonal, D., Bouriaud, O., Bruelheide, H.,
 695 Bussotti, F., Carnol, M., ... Schlesinger, W. H. (2016). Biotic homogenization can decrease landscape-scale forest multifunctionality. *Proceedings of the National Academy of Sciences of the United States of America*, 113(13), 3557–3562. <https://doi.org/10.1073/pnas.1517903113>
- Van Meerbeek, K., Jucker, T., & Svenning, J. C. (2021). Unifying the concepts of stability and resilience in ecology. *Journal of Ecology*, March, 1–19. <https://doi.org/10.1111/1365-2745.13651>
- 700 Van Passel, J., Bernardino, P. N., Lhermitte, S., Rius, B. F., Hirota, M., Conradi, T., De Keersmaecker, W., Van Meerbeek, K., & Somers, B. (2024a). Critical slowing down of the Amazon forest after increased drought occurrence. *Proceedings of the National Academy of Sciences*, 121(22), e2316924121. <https://doi.org/10.1073/pnas.2316924121>



- Van Passel, J., Bernardino, P. N., Lhermitte, S., Rius, B., Hirota, M., Conradi, T., De Keersmaecker, W., Van Meerbeek, K., & Somers, B. (2024b). Critical slowing down of the Amazon forest after increased drought occurrence (p. 200326191 Bytes) [Dataset]. figshare. <https://doi.org/10.6084/M9.FIGSHARE.24220537.V2>
- Van Passel, J., De Keersmaecker, W., Bernardino, P. N., Jing, X., Umlauf, N., Van Meerbeek, K., & Somers, B. (2022). Climatic legacy effects on the drought response of the Amazon rainforest. *Global Change Biology*, 28(19), 5808–5819. <https://doi.org/10.1111/gcb.16336>
- Venables, W. N., & Ripley, B. D. (2002). *Modern Applied Statistics with S* (Fourth). Springer. <https://www.stats.ox.ac.uk/pub/MASS4/>
- Walsh, P. D., & Lawler, D. M. (1981). Rainfall seasonality: Description, spatial patterns and change through time. *Weather*, 36, 201–208.
- Wang, S., & Loreau, M. (2016). Biodiversity and ecosystem stability across scales in metacommunities. *Ecology Letters*, 19(5), 510–518. <https://doi.org/10.1111/ele.12582>
- Wu, D., Vargas G., G., Powers, J. S., McDowell, N. G., Becknell, J. M., Pérez-Aviles, D., Medvigy, D., Liu, Y., Katul, G. G., Calvo-Alvarado, J. C., Calvo-Obando, A., Sanchez-Azofeifa, A., & Xu, X. (2022). Reduced ecosystem resilience quantifies fine-scale heterogeneity in tropical forest mortality responses to drought. *Global Change Biology*, 28(6), 2081–2094. <https://doi.org/10.1111/gcb.16046>
- Wu, J., Kobayashi, H., Stark, S. C., Meng, R., Guan, K., Tran, N. N., Gao, S., Yang, W., Restrepo-Coupe, N., Miura, T., Oliviera, R. C., Rogers, A., Dye, D. G., Nelson, B. W., Serbin, S. P., Huete, A. R., & Saleska, S. R. (2018). Biological processes dominate seasonality of remotely sensed canopy greenness in an Amazon evergreen forest. *New Phytologist*, 217(4), 1507–1520. <https://doi.org/10.1111/nph.14939>
- Yachi, S., & Loreau, M. (1999). Biodiversity and ecosystem productivity in a fluctuating environment: The insurance hypothesis. *Proceedings of the National Academy of Sciences*, 96(4), 1463–1468. <https://doi.org/10.1073/pnas.96.4.1463>
- Zemp, D. C., Schleussner, C. F., Barbosa, H. M. J., Hirota, M., Montade, V., Sampaio, G., Staal, A., Wang-Erlandsson, L., & Rammig, A. (2017). Self-amplified Amazon forest loss due to vegetation-atmosphere feedbacks. *Nature Communications*, 8, 10. <https://doi.org/10.1038/ncomms14681>
- Zuquim, G., Van Doninck, J., Chaves, P. P., Quesada, C. A., Ruokolainen, K., & Tuomisto, H. (2023). Introducing a map of soil base cation concentration, an ecologically relevant GIS-layer for Amazonian forests. *Geoderma Regional*, 33, e00645. <https://doi.org/10.1016/j.geodrs.2023.e00645>